



HAL
open science

Sulfur single-wavelength anomalous diffraction crystal structure of a pheromone-binding protein from the honeybee *Apis mellifera* L.

Audrey Lartigue, Arnaud Gruez, Loïc Briand, Florence Blon, Valérie Bézirard, Martin Walsh, J Claude Pernollet, Mariella Tegoni, Christian Cambillau

► To cite this version:

Audrey Lartigue, Arnaud Gruez, Loïc Briand, Florence Blon, Valérie Bézirard, et al.. Sulfur single-wavelength anomalous diffraction crystal structure of a pheromone-binding protein from the honeybee *Apis mellifera* L.. *Journal of Biological Chemistry*, 2004, 279 (6), pp.4459-4464. 10.1074/jbc.M311212200 . hal-02682525

HAL Id: hal-02682525

<https://hal.inrae.fr/hal-02682525v1>

Submitted on 1 Jun 2020

HAL is a multi-disciplinary open access archive for the deposit and dissemination of scientific research documents, whether they are published or not. The documents may come from teaching and research institutions in France or abroad, or from public or private research centers.

L'archive ouverte pluridisciplinaire **HAL**, est destinée au dépôt et à la diffusion de documents scientifiques de niveau recherche, publiés ou non, émanant des établissements d'enseignement et de recherche français ou étrangers, des laboratoires publics ou privés.

Sulfur Single-wavelength Anomalous Diffraction Crystal Structure of a Pheromone-Binding Protein from the Honeybee *Apis mellifera* L*

Received for publication, October 13, 2003, and in revised form, October 31, 2003
Published, JBC Papers in Press, October 31, 2003, DOI 10.1074/jbc.M311212200

Audrey Lartigue‡§, Arnaud Gruez‡, Loïc Briand¶, Florence Blon¶, Valérie Bézirard¶, Martin Walsh||, Jean-Claude Pernollet¶, Mariella Tegoni‡, and Christian Cambillau‡**

From the ‡Architecture et Fonction des Macromolécules Biologiques, Unite Mixte de Recherche 6098 CNRS and Universités Aix-Marseille I and II, 13402 Marseille Cedex 20, France, ¶Biochimie et Structure des Protéines, Unité de Recherches Institut National de la Recherche Agronomique 477, Domaine de Vilvert, F-78352 Jouy-en-Josas Cedex, France, and ||Medical Research Council France, European Synchrotron Radiation Facility, B. P. 220, F-38043 Grenoble Cedex, France

Pheromone binding proteins (PBPs) are small helical proteins (~13–17 kDa) present in several sensory organs from moth and other insect species. They are involved in the transport of pheromones from the sensillar lymph to the olfactory receptors. We report here the crystal structure of a PBP (Amel-ASP1) originating from the honeybee (*Apis mellifera*) antennae and expressed as recombinant protein in the yeast *Pichia pastoris*. Crystals of Amel-ASP1 were obtained at pH 5.5 using the nanodrops technique of crystallization with a novel optimization procedure, and the structure was solved initially with the single-wavelength anomalous diffraction technique using sulfur anomalous dispersion. The structure of Amel-ASP1 has been refined at 1.6-Å resolution. Its fold is roughly similar to that of other PBP/odorant binding proteins, presenting six helices and three disulfide bridges. Contrary to the PBPs from *Bombyx mori* (Sandler, B. H., Nikonova, L., Leal, W. S., and Clardy, J. (2000) *Chem. Biol.* 7, 143–151) and *Leucophaea maderae* (Lartigue, A., Gruez, A., Spinelli, S., Riviere, S., Brossut, R., Tegoni, M., and Cambillau, C. (2003) *J. Biol. Chem.* 278, 30213–30218), the extended C terminus folds into the protein and forms a wall of the internal hydrophobic cavity. Its backbone groups establish two hydrogen bonds with a serendipitous ligand, *n*-butyl-benzene-sulfonamide, an additive used in plastics. This mode of binding might, however, mimic that used by one of the pheromonal blend components and illustrates the binding versatility of PBPs.

Honeybees, like most insects, use small signaling chemical compounds to recognize and respond to their environment and to congeneric animals. In insects, odorant binding proteins (OBPs)¹ are small helical proteins, which ferry these com-

pounds from air to the olfactory receptors through the sensillar lymph (1, 2). Pheromone binding proteins (PBP) are a sub-class of OBPs which carry pheromonal molecules to their receptors, which then induce sexual or endocrine responses to cognates (3).

In the honeybee antennae, three different classes of antennal-specific proteins (ASPs) have been identified as OBPs: ASP1, ASP2, and ASP3 (4). ASP2 was assigned to be a general odorant binding protein (5), whereas ASP3 was classified as a chemosensory protein (6). The blend corresponding to the major components of the queen bee mandibular gland extract is composed of 9-keto-2(E)-decanoic acid (9-ODA; 68.5%), 9-hydroxy-2(E)-decanoic acid (9-HDA R(-) or S(+); 25%), methyl *p*-hydroxybenzoate (6%), and 4-hydroxy-3-methoxyphenylethanol (0.5%), as defined for the average amount of pheromone found in the gland of mated queen (7). *Apis mellifera* ASP1 (Amel-ASP1) was shown to be associated with the queen pheromone detection and able to bind 9-ODA and 9-HDA, the most active components of the queen pheromone blend (8). Amel-ASP1 should, therefore, be considered as an hymenopteran PBP.

To date, three three-dimensional structures of insect OBP/PBPs are available: the first, originating from the Lepidopteran *Bombyx mori* (BmorPBP), has been solved free or in complex with its pheromone bombykol, an alkyl unsaturated alcohol (9–11). This crystallographic structure revealed a new α -helical fold delineating a buried cavity filled with bombykol. Two three-dimensional structures of the apo-protein were further solved by NMR (11, 12). The one at low pH (pH 4.5) revealed that the C terminus (residues 125–137) has switched from an elongated stretch conformation to an α -helix. Amazingly, this 7th helix occupies the internal cavity filled with bombykol in the x-ray structure of the complex (12). In contrast, the other apo-form solved at neutral pH exhibits a three-dimensional structure close to that observed by x-ray diffraction in the complex, confirming thus the importance of the pH in triggering the 7th helix formation and internalization (11). The structure of a PBP from a cockroach, *Leucophaea maderae* (LmaPBP), has been solved free or in complex with a component of the pheromonal blend. Its structure with a fluorescence probe, 1-anilino-8-naphthalenesulfonate, definitely assessed that the PBP cavity is titrated when performing probe-chasing ligand

* This study was supported in part by the Conseil Général des Bouches-du-Rhône and by the Genopoles program.

The atomic coordinates and structure factors (code 1R5R) have been deposited in the Protein Data Bank, Research Collaboratory for Structural Bioinformatics, Rutgers University, New Brunswick, NJ (<http://www.rcsb.org/>).

§ A recipient of PACA region PhD Grant 9811/2177. The costs of publication of this article were defrayed in part by the payment of page charges. This article must therefore be hereby marked "advertisement" in accordance with 18 U.S.C. Section 1734 solely to indicate this fact.

** To whom correspondence should be addressed. Tel.: 33-49116-4501; Fax: 33-49116-4536; E-mail: cambillau@afmb.cnrs-mrs.fr.

¹ The abbreviations used are: OBP, odorant binding protein; PBP, pheromone binding protein; ASP, antennal-specific proteins; 9-ODA,

9-keto-2(E)-decanoic acid; 9-HDA R(-) or S(+), 9-hydroxy-2(E)-decanoic acid; BmorPBP, Lepidopteran *Bombyx mori* PBP; LmaPBP, PBP from *Leucophaea maderae*; SAD, single-wavelength anomalous diffraction; ESRF, European Synchrotron Radiation Facility; GC/MS, gas chromatography coupled mass spectroscopy.

TABLE I
 Data reduction and refinement statistics

Values in parentheses are for the highest resolution shell. RMSD, root-mean-square deviation; n.a., not applicable.

X-ray source	ID14-EH2	BM14
Data set		
λ (Å)	0.933	1.7712
f''	n.a.	0.7188
Total rotation range	110°	954°
Reflections observed	188,214	225188
Unique reflections	22,274	6433
Resolution (Å)	28–1.6 (1.7–1.6)	50.0–2.4 (2.5–2.4)
R_{sym} (%)	3.6 (26.7)	7.6 (33.0)
$I/\sigma(I)$	10.2 (2.6)	75.0 (9.0)
Completeness	99.7 (99.7)	96.4 (62.6)
Multiplicity	3.8 (3.8)	35.0 (15.5)
Refinement		
Resolution (Å)	20–1.6 (1.6–1.64)	
Reflections	19,845	
Number of protein/ligand/water atoms	1074/14/154	
$R_{\text{work}}/R_{\text{free}}$	0.173/0.208	
RMSD bonds(Å)/angles(°)	0.014/1.49	
Average B factors (molecule/ligand/water)	21.0/43.4/43.6	
Procheck zones 1 & 2 (%)	91.3, 7.7	

studies (13). LmaPBP structure ends just after the sixth helix (helix F) and does not possess the amino acid stretch that forms the 7th internalized helix in BmorPBP. It has been proposed that the formation of the 7th internalized helix at low pH might mimic the physiological mechanism. The low pH observed near the cell membrane might provoke the PBP conformational change and expel the pheromone in the vicinity of the receptor. In LmaPBP, the absence of the amino acid stretch corresponding to this 7th helix together with evidence of a hydrophilic cavity binding a hydrophilic ligand suggested that a simpler mechanism of ligand binding and release might be used.

Recently, the structure of the gene product of the *Drosophila melanogaster lush* gene has been solved in complex with short chain (C2–C4) alcohols (14). The Lush phenotype is characterized by the lack of avoidance toward high concentrations of short alcohols (15). In the absence of the *lush* gene, the OBP that binds the short alcohols in the antennal lymph is not expressed and, therefore, their presence is not transmitted to the olfactory receptor. Another example of function associated with PBP/OBPs was reported by Krieger and Ross (16) who identified in *Solenopsis invicta* (fire ants) two PBP alleles regulating alternative social behaviors. Their findings indicate that, at a molecular level, different receptors might be activated by a specific PBP allele in complex with the social pheromone. These two studies, structural and functional, are milestones concerning the role of OBPs/PBPs in receptor triggering.

Here we report the crystal structure of Amel-ASP1, a protein of 13,180 Da. The crystals were obtained at pH 5.5 using the nano-drop crystallization technique (17), which was first developed to respond to the high demand of structural genomics programs, followed by a novel optimization procedure (18). The crystals diffract to 1.6 Å at synchrotron sources, and the structure was solved initially with the SAD technique using sulfur anomalous dispersion. A serendipitous ligand, *n*-butyl-benzene-sulfonamide, was found in the cavity and identified by mass spectroscopy. This molecule, used as a plasticizer in polymers such as nylon polyacetyls and polycarbonates, was probably extracted during protein preparation. This illustrates the binding versatility of PBP/OBPs (19) and further suggests that receptor triggering is based on a more subtle mechanism than specific binding of a unique signaling molecule (20).

MATERIALS AND METHODS

Amel-ASP1 Expression and Purification—Amel-ASP1 was expressed recombinant in *Pichia pastoris* and purified by reverse-phase chromatography as described previously (8). Purified protein was concentrated

(Nanosep-3, Filtron) and washed with 10 mM Tris-HCl and 25 mM NaCl, pH 8.0 to a concentration of 40 mg/ml, which was determined by spectrophotometry using the theoretical $\epsilon_{280} = 15,580 \text{ M}^{-1} \text{ cm}^{-1}$.

Crystallization of Amel-ASP1—Screening experiments were performed with several commercial kits (see Sulzenbacher *et al.* (17) for details). The nano-L crystallization experiments were performed by using the sitting drop method in Greiner plates (21). The initial crystallization droplet contained 200 nl of a 40 mg/ml protein solution in Tris 10 mM, NaCl 25 mM, pH 8.0, mixed with 100 nl of well solution containing 1.5 M ammonium sulfate, 0.15 M sodium citrate at pH 5.5. First, thin crystals of $\sim 0.02 \times 0.1 \times 0.5 \text{ mm}^3$ appeared after 1 to 3 weeks. Thicker crystals ($0.2 \times 0.1 \times 0.7 \text{ mm}^3$) have been obtained after optimization (18). Crystal improvement with nano-L drops was crucial because less than 3 mg of protein were available. We have tried to crystallize ASP1 with components of the pheromone blend. To date, however, all attempts to co-crystallize ASP1 with 9-ODA or 9-HDA led to small crystals not appropriate for structure determination.

Data Collection and Structure Solution—Crystals were cryo-cooled at 100K within their crystallization liquor with the addition of 25% glycerol as cryoprotectant. Diffraction images collected at the European Synchrotron Radiation Facility (ESRF, Grenoble) were indexed and integrated with DENZO (22) and scaled with SCALA (23). Amel-ASP1 crystallizes in space group C222₁ with cell dimensions $a = 74.8 \text{ Å}$, $b = 85.8 \text{ Å}$, and $c = 50.2 \text{ Å}$. With one molecule in the asymmetric unit, the V_m is $3.05 \text{ Å}^3/\text{Da}$, corresponding to a solvent content of 60% (24). Crystals obtained from optimized nano-drops were collected at 1.6-Å resolution on beam line ID14–2 at ESRF (Grenoble) with an ADSC-Q4 detector (Table I).

All attempts failed to solve the structure with molecular replacement methods using homologous models (the PBPs of *L. maderae* and *B. mori*). In addition, multiple isomorphous replacement or gas diffusion with Xenon also failed to provide a derivative. Se labeling was also tried (25), but the Se-labeled protein failed to crystallize. Therefore, we decided to try the SAD-phasing method at remote wavelengths using sulfur atom anomalous dispersion with native crystals. A strong theoretical Bijvoet ratio of 1.12% is expected from the 10 sulfur atoms of the protein that contribute to the anomalous signal at an x-ray wavelength of 1.77 Å. The sulfur-SAD data set was collected on beam line BM14 at ESRF, Grenoble, with an MAR charge-coupled device detector. The wavelength and the distance crystal detector were optimized to 1.77 Å and 73 mm, respectively, and a redundant data set was collected at 2.5-Å resolution. It includes 1308 images of 0.5° rotation, corresponding to 654°, completed by 300 images (300°) collected after a rotation of $\sim 15^\circ$ of the goniostat κ angle (Table I).

Data were integrated and scaled with HKL2000 and Scalepack (22). The data collection was followed with the XPREP program (26) to estimate the anomalous signal *versus* the redundancy. Five sulfur atom sites were found by using either SHELXD (27) or SOLVE (28) to 3.5-Å resolution. The quality of the phases was good enough (FOM = 0.67 for all reflections) to obtain an interpretable map at 3.5-Å resolution after solvent flattening using RESOLVE (Ref. 28; Fig. 1A). The identified location of the three disulfide bridges as well as two methionines (of the

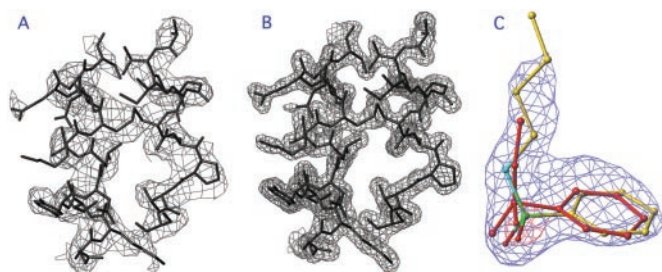


FIG. 1. **Amel-ASP1 electron density maps.** *A*, the $2F_o - F_c$ electron density map at 2.4-Å resolution after RESOLVE (28). A part of the final model is represented inside. *B*, the $2F_o - F_c$ electron density map at 1.6-Å resolution of the same part of the molecule after refinement. *C*, the $2F_o - F_c$ electron density map around the ligand area at 2.0-Å resolution after the initial refinement and before including the ligand in refinement. The electron density map contoured at 1σ and 3σ is shown in blue and red, respectively. The molecule in red is the tentative topological assignment performed according to the electron density shape. The final *n*-butyl-benzene-sulfonamide position is represented in atom-coloring mode. Note that the sulfur atom position is at the center of the 3σ -contoured electron density map. The pictures were drawn with Turbo-Frodo (30).

four expected) enabled us to build manually 52% of the model. This first model was subsequently used to extend the phases to 1.6 Å using a native data set collected on ID14-EH2 (18) and to build 85% of the structure using ARP/wARP (29). The missing parts were introduced manually with Turbo-Frodo (30). 144 water molecules were added with ARP/WARP. The structure was refined by using REFMAC (Ref. 31; see Fig. 2*B*). A serendipitous ligand was included in the refinement after GC/MS identification (see above, and see Fig. 2*C*). The final *R* and R_{free} are 17.6 and 21.2%, respectively. The coordinates and structure factors have been deposited in the Protein Data Bank under code 1R5R.

Determination of Amel-ASP1 Serendipitous Ligand Structure—Approximately 625 μg of Amel-ASP1 (50 μl) was first denatured with 100 μl of 9 M GuCl by 21-h incubation in a sealed tube at 35 °C. Amel-ASP1 was then digested with 750 μl of 30% (w/w) proteinase K (Sigma) in 50 mM phosphate buffer, pH 8.0 by overnight incubation at 35 °C. The reaction mixture was then placed on ice and extracted with 50 μl of CHCl₃. After centrifugation at 10,000 × *g* for 30 min at 4 °C, the extract was analyzed by GC/MS. Aliquots of ammonium acetate buffer (50 μl) treated in the same way were analyzed by GC/MS as blank.

Ligand analyses were conducted on a gas chromatograph (6890N, Agilent Technologies) coupled to a mass spectrometer detector (5973N, Agilent Technologies). Samples (2 μl) were injected into a non-polar capillary column (HP-5MS, 30 m × 0.25 mm, 0.25-μm film thickness, Agilent Technologies). The column was directly connected to the mass-sensitive detector by an interface heated at 280 °C. The electron impact energy was set at 70 eV, and mass spectra were recorded in the range of 20–800 atomic mass units.

RESULTS AND DISCUSSION

Sulfur-SAD Structure Resolution—Sulfur-SAD sulfur phasing has been recently tried with success on a few known or unknown structures (32–34). Amel-ASP1 possesses a large number of sulfur atoms: six in cysteines involved in SS-bridges and four in methionines. An extra sulfur atom is provided by the co-purified ligand. Eleven sulfur atoms for ~13 kDa is a favorable situation. Besides the high redundancy, no special tricks were used for data collection: oscillations of 0.5° (*versus* 0.1–0.2° used for difficult cases), a single pass of which provided most of the data, and medium resolution data (2.4 Å). The structure solution was easy to obtain; this indicates that for small to medium proteins (100–200 residues) with a ratio kDa/S-atom of ~1, sulfur-SAD should be the method of choice for obtaining the initial phases.

Overall Structure—Amel-ASP1 has been found to be a dimer in solution at pH 7.5 (8). However, a monomer is contained in the asymmetric unit at the crystallization pH of ~5.5. Another symmetry-related molecule was found to share an interface accessible surface area of 445 Å², representing 7% of the total molecular surface. This value is too low to allow that the dimer

is formed in solution in all environments and conditions. Furthermore, main contacts involved ion pairs of residues Arg-19, His-24, and Asp-61, which may depend on pH.

Amel-ASP1 polypeptide chain was readily built in the electron density map between residues 3 and 119. In addition, 144 water molecules and a serendipitous ligand, *N*-butyl-benzene-sulfonamide, were identified and introduced. Overall, the B-factors are quite low, with an average value of 21.0 Å³/Da (Table I). Amel-ASP1 is formed of six helices as are the other PBPs; as seen in Fig. 2*A*, these are located between residues 7–24 (A), 28–35 (B), 43–55 (C), 67–72 (D), 79–89 (E), and 97–111 (F). The three classical PBPs disulfide bridges are observed between Cys-20–51, Cys-47–98, and Cys-87–107, locking together helices A and C, C and F, and E and F, respectively. Three irregular, independent β-strands are formed by residues 36–46, 91–95, and 114–119 at the C terminus. A quasi β-hairpin structure (extended-turn-extended) is also observed between residues 58–66. In contrast with Bmor-PBP and LmaPBP, the extended C terminus folds inside the internal cavity, along one of its wall (see below).

The Cavity and the Bound Serendipitous Ligand—An L-shaped cavity is observed inside the protein, open wide to the solvent and filled in part by a ligand (see Fig. 2, *B* and *C*). One wall of the cavity is lined by the C terminus segment between residues 116 and 119. Pro-113 is located just after helix F (finishing at residue 111), re-orientating the polypeptide inside the protein. The last residue at the surface is Asp-114 and is followed by five hydrophobic residues: Val-115, part of the protein core, and by Trp-116, Phe-117, Val-118, and Leu-119, forming one of the internal cavity walls (see Fig. 2*C*). The rest of the cavity is covered exclusively by hydrophobic residues: Val-13, Met-49, Leu-53, Leu-74, Met-86, and Tyr-102. Val-9, Ala-55, Phe-56, Leu-58, and Leu-78 are located in the second branch of the L, which is closer to the cavity mouth. The lips of the cavity instead are formed of mixed types of residues: Trp-4, Pro-6 and -7, Glu-8, Leu-12, Asp-16, Ser-57, Leu-73, and Pro-75.

To identify the ligand initially, we have built a pseudo-molecule taking into account the shape of the electron density map. The resulting entity consisted of a phenyl ring, a tetrahedral moiety, and a short alkyl chain (Fig. 1*C*, red), a structure close to that of the identified ligand (Fig. 2*B*). Ligand identification was performed by gas chromatography coupled mass spectroscopy (GC/MS). Amel-ASP1 was denatured and digested with proteinase K to liberate the noncovalently bound ligand. A CHCl₃ extract of the digest analyzed by gas chromatography yielded a prominent peak (Fig. 3*A*). Comparison of control and Amel-ASP1 showed a single peak difference in mass spectra. After comparison with the National Institute of Standards and Technology library of mass spectra, the electronic impact mass spectrum of this compound (M^+ 213 plus characteristic ions at *m/z* 77, 141, 170) was found to correspond to an *n*-butyl-benzene-sulfonamide molecule (Fig. 3*B*).

The shape of the serendipitous ligand, *n*-butyl-benzene-sulfonamide, fits well the cavity L-shape. Its B-factors are two times higher than those of the protein on average (39.9 Å³/Da *versus* 21.0 Å³/Da). Intriguingly, the phenyl ring is facing the bulk solvent in the cavity opening, whereas the polar SO₂ and *N*-butyl moieties are more buried (Fig. 2*B*). One of the S=O group and the *N*-H group are engaged in hydrogen bonds with the C terminus backbone, the *N*-H group of Leu-119 (3.0 Å) and the C=O group of Phe-117 (2.6 Å), respectively (Fig. 2*C*). Besides these two strong and well oriented hydrogen bonds, the interactions are hydrophobic.

Comparison with other PBPs and Functional Implications—Amel-ASP1 is the fourth PBP crystal structure available to

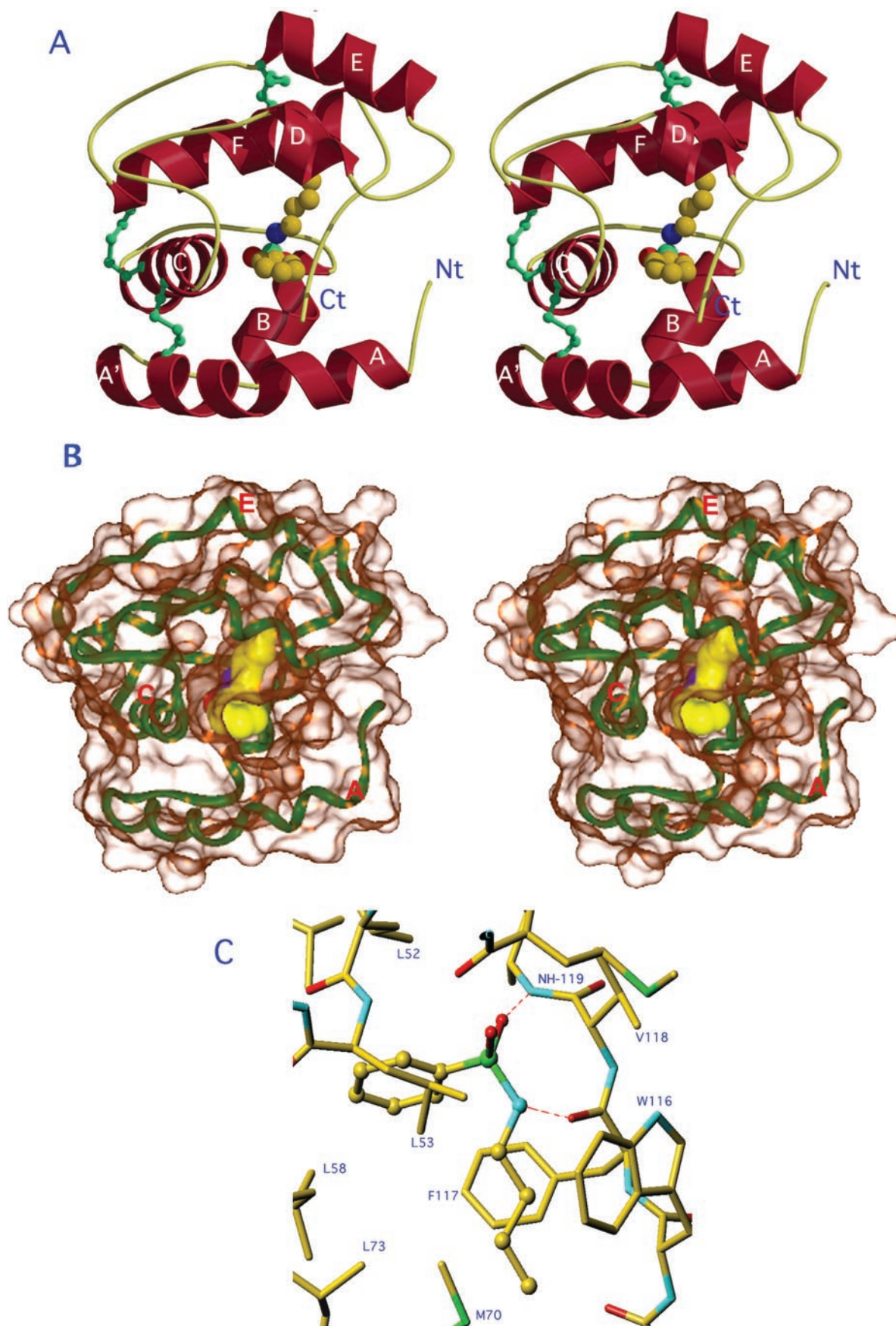


FIG. 2. **The three-dimensional structure of Amel-ASP1.** *A*, stereo view of the PBP Ca trace (represented as *ribbons*) of the disulfide bridges and of the ligand, *n*-butyl-benzene-sulfonamide. The helices are labeled A–F from N to C terminus. *B*, stereo ribbon view of Amel-ASP1 (*blue*) with its surface represented as transparent and the same orientation as in *A*. The shape of the cavity is visible inside as well as the ligand. Helices A, C, and E have been identified. Note the phenyl ring facing the cavity opening. *C*, close-up of the ligand in the binding site. The hydrogen bonds with C terminus residues are identified by a *dashed red line*. A few residues of the slatted binding site are identified. The pictures were drawn with Molscript (38) and Turbo-Frodo (30).

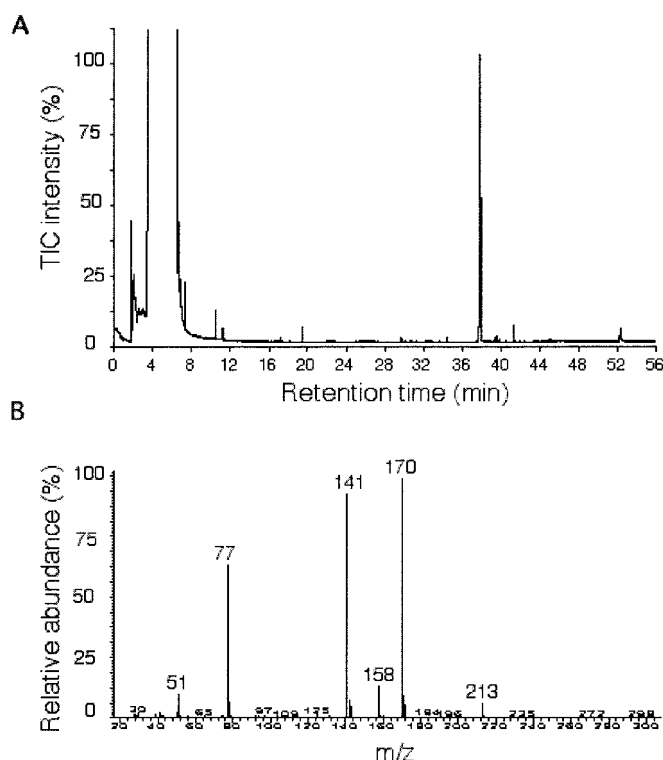


FIG. 3. Identification of ligand extracted from AmelASP1 by gas chromatography-coupled mass spectrometry. *A*, gas chromatogram of CHCl₃ extract of AmelASP1 displaying a prominent peak. *B*, mass spectra of the main peak identified as *n*-butyl-benzene-sulfonamide.

date. Its root-mean-square deviations toward the other three structures vary between 1.9 and 2.2 Å for 110 residues included in the comparison. The closest is Lush, with a root-mean-square deviation of 1.9 Å; the others display root-mean-square deviation values of 2.2 Å. Many conformational changes are observed between these four structures (Fig. 4). The most significant are, indeed, at the C terminus: the shortest, LmaPBP, has no C-terminal stretch and stops at the protein surface just after helix F. BmorPBP has a long C terminus, is elongated on the protein surface in the presence of the ligand and at neutral pH, and folds as a 7th helix inside the protein at acidic pH. Both Lush and Amel-ASP1 possess a short, extended irregular β -structure that folds inside the protein and forms one wall of the cavity (residues 119–124 and 113–117, respectively).

In the three previously solved PBP structures, the cavity walls are hydrophobic but also possess a few polar residues: Ser-56 in BmorPBP, Ser-52 and Thr-57 in Lush, and Tyr-5, Tyr-75, and Thr-111 in LmaPBP. These residues are used to anchor the pheromones or odors which all bear polar groups: bombykol, EtOH/butanol, and 3-hydroxy-butan-2-1, respectively. The cavities of the two closest structures, those of Lush and Amel-ASP1, present some analogy because of the presence of the C terminus inside. However, whereas the cavity of Amel-ASP1 is totally hydrophobic, that of Lush presents polar residues such as Ser-52 and Thr-57. Ser-52 is replaced by Leu-53 in Amel-ASP1, whereas Thr-57 has no topological equivalent because their backbones follow different tracks in this region. In Amel-ASP1, therefore, the hydrogen bonds with the ligand are established with backbone groups. Another striking difference between the two latter PBPs is the position of helix A, which is displaced 3–4 Å toward solvent relative to that of Lush (Fig. 4). This displacement also influences the position of the first disulfide bridge, whose position is 4 Å from that of Lush. Consequently, the cavity of Amel-ASP1 is larger than that of Lush,

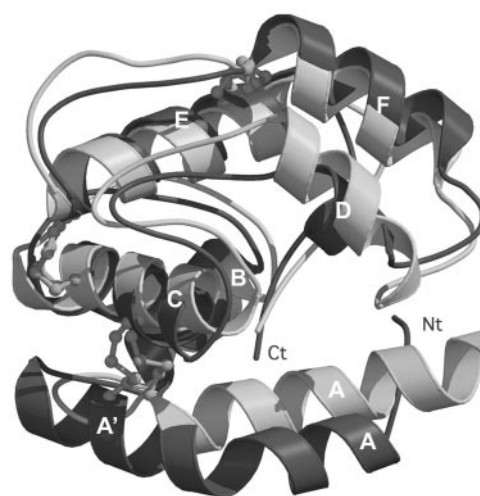


FIG. 4. View of the superposition between the OBP Lush (light gray) and Amel-ASP1 (dark gray). The two striking features are the position of their N termini and the external position of helix A in Amel-ASP1 compared with Lush. The picture was drawn with Mol-script (38).

because the other secondary structure elements have similar positions.

The four components of the pheromonal blend of Amel-ASP1 all possess polar groups. The two main components, ODA and HAD, have been found to bind to Amel-ASP1 but not to the two other honeybee antennal proteins, thus identifying Amel-ASP1 as a PBP. They possess a carboxylic group at one extremity, and a keto or hydroxyl group on the penultimate atom. Neither the cavity nor the cavity mouth bears any positively charged Lys, Arg, or His to accommodate the carboxylic group. It may be postulated that this group is simply exposed to the bulk solvent. Concerning the penultimate keto or hydroxyl groups, they might establish a hydrogen bond to the backbone N-H group of Leu-119. The rest of the molecule would be nicely accommodated by aromatic/hydrophobic residues of the cavity.

Concluding Remarks—Amazingly, although PBPs display a similar fold, the diverse positions, lengths, and orientations of their helices provide a rather versatile scaffold. An additional element of this diversity is the wide variety of the loops. In contrast, the positions of the disulfide bridges are on average more conserved than the rest of the proteins. All of these features result in proteins having very different cavity shapes or nature (hydrophilic versus hydrophobic); hence, they are able to accommodate a large range of organic compounds. A single PBP has also been shown capable of accommodating various compounds with μ M affinities, including fluorescent probes (19). LmaPBP exhibits a side-chain flexibility that permits the cavity to adapt to bulky ligands (13). This versatility is confirmed with Amel-ASP1; a serendipitous ligand has been found in its cavity. The presence of functional or serendipitous ligands has been reported for several classes of lipid-binding proteins such as lipocalins (35) or the binding domain of nuclear receptors (36). In the case of PBPs, it has been proposed that, although they are able to bind several compounds (19), only the functional ligand would be able to let them achieve the conformation that would trigger their receptor. Such subtle conformational changes have been detected by using circular dichroism and differential spectroscopy (20, 37). Because several structures of PBPs are available at present, the challenge now is to document these subtle conformational changes.

REFERENCES

- Vogt, R. G., Prestwich, G. D., and Lerner, M. R. (1991) *J. Neurobiol.* **22**, 74–84
- Vogt, R. G., and Riddiford, L. M. (1981) *Nature* **293**, 161–163

3. Krieger, J., von Nickisch-Rosenegk, E., Mameli, M., Pelosi, P., and Breer, H. (1996) *Insect Biochem. Mol. Biol.* **26**, 297–307
4. Danty, E., Arnold, G., Huet, J. C., Huet, D., Masson, C., and Pernollet, J. C. (1998) *Chem. Senses* **23**, 83–91
5. Briand, L., Nespoulous, C., Huet, J. C., Takahashi, M., and Pernollet, J. C. (2001) *Eur. J. Biochem.* **268**, 752–760
6. Briand, L., Swasdipan, N., Nespoulous, C., Bezirard, V., Blon, F., Huet, J. C., Ebert, P., and Penollet, J. C. (2002) *Eur. J. Biochem.* **269**, 4586–4596
7. Slessor, K. N., Kaminski, L. A., King, G. G. S., Borden, J. H., and Winston, M. L. (1988) *Nature* **332**, 354–356
8. Danty, E., Briand, L., Michard-Vanhee, C., Perez, V., Arnold, G., Gaudemer, O., Huet, D., Huet, J. C., Ouali, C., Masson, C., and Pernollet, J. C. (1999) *J. Neurosci.* **19**, 7468–7475
9. Sandler, B. H., Nikonova, L., Leal, W. S., and Clardy, J. (2000) *Chem. Biol.* **7**, 143–151
10. Horst, R., Damberger, F., Peng, G., Nikonova, L., Leal, W. S., and Wuthrich, K. (2001) *J. Biomol. NMR* **19**, 79–80
11. Lee, D., Damberger, F. F., Peng, G., Horst, R., Guntert, P., Nikonova, L., Leal, W. S., and Wuthrich, K. (2002) *FEBS Lett.* **531**, 314–318
12. Horst, R., Damberger, F., Luginbuhl, P., Guntert, P., Peng, G., Nikonova, L., Leal, W. S., and Wuthrich, K. (2001) *Proc. Natl. Acad. Sci. U. S. A.* **98**, 14374–14379
13. Lartigue, A., Gruez, A., Spinelli, S., Riviere, S., Brossut, R., Tegoni, M., and Cambillau, C. (2003) *J. Biol. Chem.* **278**, 30213–30218
14. Kruse, S. W., Zhao, R., Smith, D. P., and Jones, D. N. (2003) *Nat. Struct. Biol.* **10**, 694–700
15. Kim, M. S., and Smith, D. P. (2001) *Chem. Senses* **26**, 195–199
16. Krieger, M. J., and Ross, K. G. (2002) *Science* **295**, 328–332
17. Sulzenbacher, G., Gruez, A., Roig-Zamboni, V., Spinelli, S., Valencia, C., Pagot, F., Vincentelli, R., Bignon, C., Salomoni, A., Grisel, S., Maurin, D., Huyghe, C., Johansson, K., Grassick, A., Roussel, A., Bourne, Y., Perrier, S., Miallau, L., Cantau, P., Blanc, E., Genevois, M., Grossi, A., Zenatti, A., Campanacci, V., and Cambillau, C. (2002) *Acta Crystallogr. Sect. D Biol. Crystallogr.* **58**, 2109–2115
18. Lartigue, A., Gruez, A., Briand, L., Pernollet, J. C., Spinelli, S., Tegoni, M., and Cambillau, C. (2003) *Acta Crystallogr. Sect. D Biol. Crystallogr.* **59**, 919–921
19. Campanacci, V., Krieger, J., Bette, S., Sturgis, J. N., Lartigue, A., Cambillau, C., Breer, H., and Tegoni, M. (2001) *J. Biol. Chem.* **276**, 20078–20084
20. Bette, S., Breer, H., and Krieger, J. (2002) *Insect Biochem. Mol. Biol.* **32**, 241–246
21. Mueller, U., Nyarsik, L., Horn, M., Rauth, H., Przewieslik, T., Saenger, W., Lehrach, H., and Eickhoff, H. (2001) *J. Biotechnol.* **85**, 7–14
22. Otwinowski, Z., and Minor, W. (1997) *Methods Enzymol.* **276**, 307–326
23. Collaborative Computational Project Number 4 (1994) *Acta Crystallogr. D* **50**, 760–763
24. Matthews, B. W. (1968) *J. Mol. Biol.* **33**, 491–497
25. Larsson, A. M., Stahlberg, J., and Jones, T. A. (2002) *Acta Crystallogr. Sect. D Biol. Crystallogr.* **58**, 346–348
26. Sheldrick, G. M., and Schneider, T. R. (2001) in *Methods in Macromolecular Crystallography* (Turk, D., and Johnson, L., eds) IOS Press, Amsterdam, The Netherlands
27. Schneider, T. R., and Sheldrick, G. M. (2002) *Acta Crystallogr. D Biol. Crystallogr.* **58**, 1772–1779
28. Terwilliger, T. C. (2000) *Acta Crystallogr. Sect. D Biol. Crystallogr.* **56**, Part 8, 965–972
29. Perrakis, A., Morris, R., and Lamzin, V. S. (1999) *Nat. Struct. Biol.* **6**, 458–463
30. Roussel, A., and Cambillau, C. (1991) *Silicon Graphics Geometry Partners Directory*, Silicon Graphics, Mountain View, CA
31. Murshudov, G. N., Vagin, A. A., and Dodson, E. J. (1997) *Acta Crystallogr. Sect. D* **53**, 240–255
32. Ramagopal, U. A., Dauter, M., and Dauter, Z. (2003) *Acta Crystallogr. Sect. D Biol. Crystallogr.* **59**, 1020–1027
33. Debreczeni, J. E., Bunkoczi, G., Ma, Q., Blaser, H., and Sheldrick, G. M. (2003) *Acta Crystallogr. Sect. D Biol. Crystallogr.* **59**, 688–696
34. Debreczeni, J. E., Bunkoczi, G., Girmann, B., and Sheldrick, G. M. (2003) *Acta Crystallogr. Sect. D Biol. Crystallogr.* **59**, 393–395
35. Ramoni, R., Vincent, F., Grolli, S., Conti, V., Malosse, C., Boyer, F. D., Nagnan-Le Meillour, P., Spinelli, S., Cambillau, C., and Tegoni, M. (2001) *J. Biol. Chem.* **276**, 7150–7155
36. Potier, N., Billas, I. M., Steinmetz, A., Schaeffer, C., van Dorsselaer, A., Moras, D., and Renaud, J. P. (2003) *Protein Sci.* **12**, 725–733
37. Mohl, C., Breer, H., and Krieger, J. (2002) *Invert. Neurosci.* **4**, 165–174
38. Kraulis, P. (1991) *J. Appl. Crystallogr.* **24**, 946–950